FUSED FILAMENT FABRICATION OF RECYCLED COMPOSITES FROM GLASS FIBER WIND TURBINE WASTE: A METHODOLOGY AND FINITE ELEMENT MODEL

Zhengshu Yan[1], Amir Rahimizadeh[1], Yixue Zhang[1] and Larry Lessard[1]

[1] Department of Mechanical Engineering, McGill University, Montreal, QC, H3A 0C3, CA
larry.lessard@mcgill.ca
https://www.mcgill.ca/composite/

Keywords: Wind turbine blades, Glass fiber waste, Composite recycling, Fused filament fabrication, Representative volume element

ABSTRACT

Wind turbines play a critical role in producing clean electricity. However, the mounting number of discarded wind turbine blades has created a hazardous waste issue worldwide. To address this challenge, a novel recycling method that involves mechanical grinding and fused filament fabrication has emerged as a promising solution. This approach offers a cost-effective way to minimize waste while maintaining the improved mechanical properties of the recycled fabricated samples.

Due to the complex structure of 3D printed samples, the Representative Volume Element (RVE) is a valuable simulation model. To generate RVEs with hybrid and arbitrary-geometry reinforcements efficiently, this paper introduces a Modified Random Sequential Adsorption (MRSA) algorithm. Compared to the traditional RSA algorithm, MRSA offers the advantage of reducing computational costs associated with detecting fiber intersections. The error between Finite Element Analysis (FEA) and experimental results obtained using MRSA is lower than those obtained with the Mori-Tanaka and Halpin-Tsai methods.

1 INTRODUCTION

1.1 Recycling background

Despite being a sustainable option for electricity generation, wind energy has generated a significant amount of waste material and negative environmental impacts due to the extensive use of fiberglass in composite wind turbine blades and the rapid expansion of the wind energy sector [1, 2]. Although 85% of wind turbines, like housing and tower parts, are made of recyclable materials like steel and copper [3], non-biodegradable materials, such as fiberglass, plastic polymer, and core, are employed to construct high-performance wind turbine blades and enhance their efficiency [4]. Since turbine blades have a lifespan of 25 years, many of the first-generation turbines have already reached their end-of-life, rendering wind turbine blades a major source of composite waste [2]. Furthermore, it is predicted that the amount of waste generated annually from end-of-life wind turbine blades will surge from over 50,000 tonnes in 2021 to more than 200,000 tonnes worldwide by 2034 [5].

Mechanical grinding offers several benefits compared to traditional recycling methods such as incineration and landfilling. It is a straightforward, environmentally friendly, and economically viable method. Furthermore, mechanical grinding can effectively reduce the size of composite waste particles due to the abrasive properties of glass fibers [6]. This approach involves shredding, milling, grinding, and other size reduction processes to reduce scrap composites' size and reconstitute them as reinforcement in new composite structures [6-10].

To tackle the issue of wind turbine blade waste, Rahimizadeh et al. [11] proposed a recycling solution that combines mechanical grinding with fused filament fabrication (FFF) 3D printing (Figure 1). This approach involves a step-by-step process that produces structurally stiff and strong recycled parts. The process begins with the retrieval of discontinuous short and long glass fibers, which are coated in epoxy residue from end-of-life wind turbine blades. These fibers are then mixed with polylactic acid (PLA)

during an extrusion process to create fiber-reinforced filaments with enhanced mechanical properties (Figure 2). Finally, the filament is utilized as feedstock for FFF 3D printing applications.
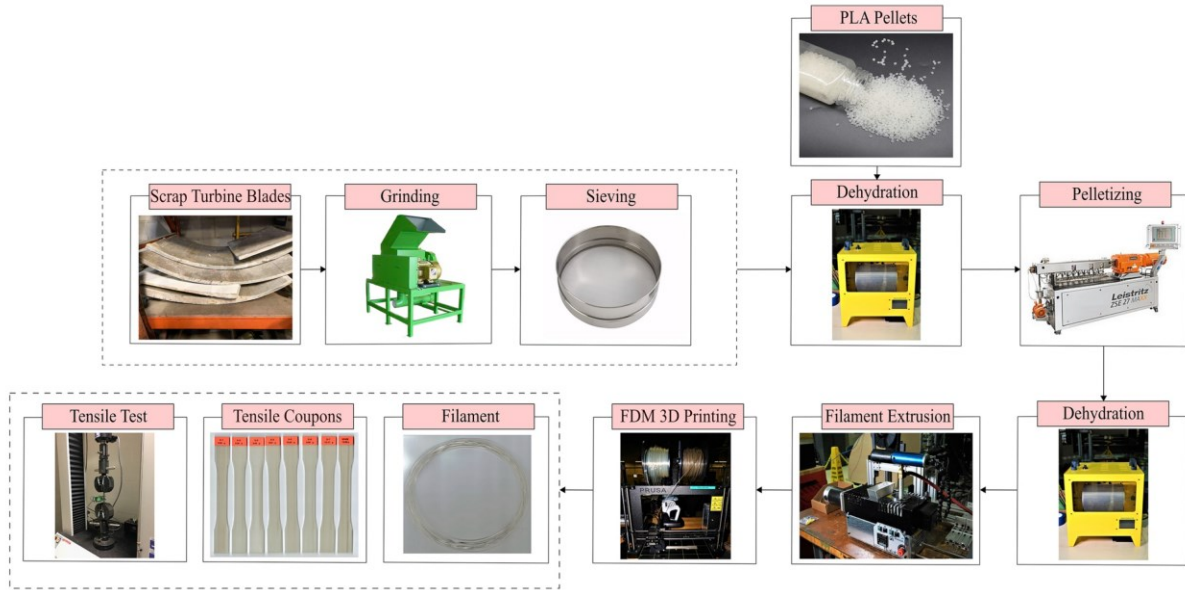

Figure 1: The proposed methodology for the recycling of wind turbine blades [11].

Rahimizadeh et al. [11, 12] conducted various mechanical tests to evaluate the performance of the recycled parts produced using the proposed recycling approach. The results revealed a promising solution for recycling end-of-life wind turbine blades, with improvements in mechanical performance and no negative environmental impact. In particular, the newly developed feedstock demonstrated up to 20% and 28% enhancement in tensile strength and stiffness, respectively, compared to pure thermoplastic feedstock materials currently available on the market.
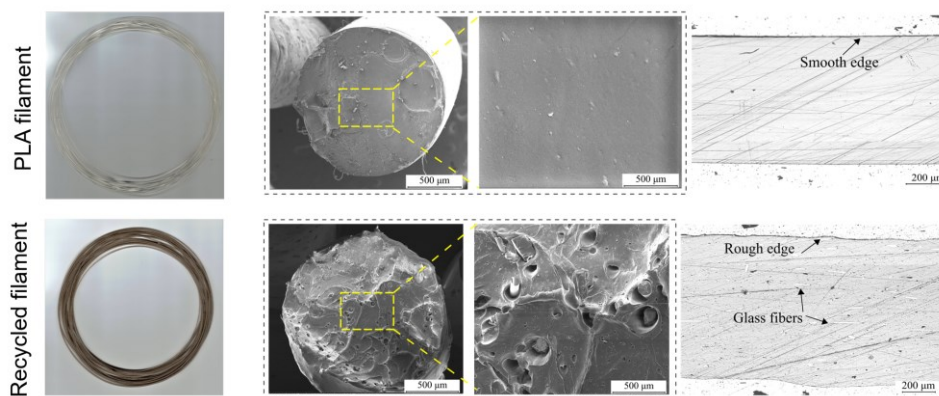

Figure 2: Pure PLA, recycled fabricated filaments, and corresponding scanning electron microscope (SEM) images [11].

1.2 Numerical simulations

Simulation models such as numerical models and finite element analysis (FEA) are essential for the design process and material assessment in the proposed recycling solution. Numerical models have the advantage of being well-studied, and there are no restrictions on the geometry, material properties, and phase angles of the composite material [13]. Mori and Tanaka's work is one of the well-known numerical models available for such simulations [14]. The material behaviour and performance of discontinuous random fiber reinforcement composites produced from this recycling solution are influenced by various factors, such as fiber aspect ratio, fiber orientation, reinforcement shape, etc [15-17]. However, the presence of voids and particles can decrease the accuracy of numerical models. In this regard, FEA can provide promising alternatives, but only if they consider all relevant aspects of the problem.

Explicitly modelling all features of a 3D-printed composite component is computationally demanding and impractical, requiring enormous computational resources to obtain a convergent solution. To circumvent this challenge, mechanical analysis methods can be utilized to determine the effective mechanical properties of the material by analyzing a representative volume element (RVE) [18]. The RVE should be of sufficient size to incorporate enough reinforcement, and its effective properties must statistically represent the material properties on a macroscopic scale [19]. However, selecting a larger RVE size increases computational cost, and therefore, a balance must be struck between computational efficiency and accuracy by minimizing the RVE size while ensuring accuracy.

To ensure accuracy, the RVE should have the same elastic constants and fiber volume fraction as the original composite. The macrostructure of a 3D printed component can be represented in three hierarchical levels, as shown in Figure 3. These levels include the extrudates, the building blocks of 3D printing with interlayer voids, and the composite compound unit.
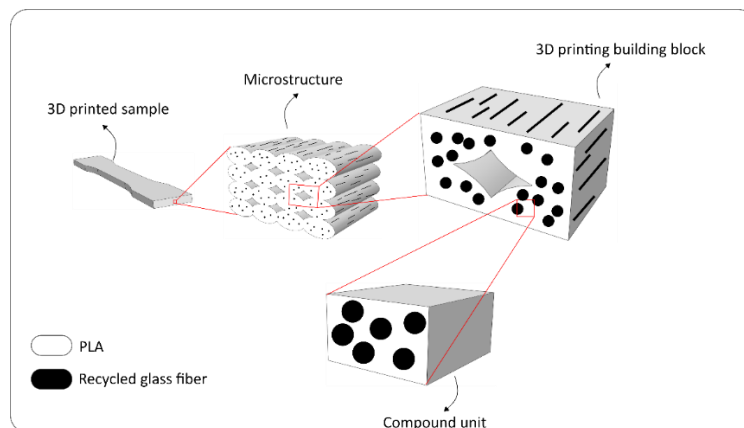

Figure 3: The 3-order hierarchical structure of a 3D printed sample.

2 PROPOSED METHODOLOGIES

2.1 Grinding and sieving

A three-stage grinding was utilized to extract fibers for filament extrusion (Figure 1). Initially, the scrap turbine blades were cut into smaller pieces (20 cm × 20 cm) and then subjected to a hammer mill system and a metal classifier with a 3 mm hole diameter. Next, a double-sieving mechanism was employed to classify the recycled materials (a mixture of fibers and resin powder) using stainless steel sieving screens with hole diameters of 1.18mm, 0.1mm, and 0.075mm, resulting in two grades of granulated materials. The larger-sized recycled material was subjected to a second sieving operation using the sieve shaker to extract more fine fibers. The residual material obtained after sieving can be recycled by either regrinding and reusing it or processing it with larger nozzle diameters.

To enhance the efficiency of the sieving process, several factors such as sieving time, sieving method, and other related parameters were investigated.

2.1.1 Sieving time

The duration of the sieving process is important for achieving optimal fiber extraction. Insufficient sieving time may result in a low recovery rate of fibers, while excessive sieving time can lead to a reduction in recovery efficiency. Furthermore, prolonged sieving can result in long fibers penetrating through the screen, causing an undesired mixing of short and long fibers.

The same batch of fibers was subjected to sieving for 10, 20, and 30 minutes to determine the optimal sieving time. The results showed that the fiber recovery increased with the duration of the sieving process, but the rate of increase gradually decreased (Figure 4). After considering the recovery efficiency and the need to avoid excessively long fibers, a sieving time of 30 minutes was determined to be appropriate.

	1.18 mm screen	0.1 mm screen	0.075 mm screen	Final	**Recovery**
10 min					**21.0%**
20 min					**28.1%**
30 min					**33.1%**

Figure 4: Sieving screens and fibers in each sieving stage after different durations of sieving.

2.1.2 Sieving method and results

Approximately 2.4 kg of ground fibers underwent the double-sieving process. The fibers that passed through the 0.075 mm screen (i.e., < 0.075 mm), which represented the "finest fibers", were collected during the first and second sieving stages. An additional sieving step was conducted, and the fibers that passed through the 0.1 mm screen but remained on or before the 0.075 mm screen (i.e., 0.075 mm to 0.1 mm), which represented the "finer fibers", were collected during the second and third sieving stages. To avoid any impact on the recovery of the finest fibers, the finer fibers were not collected during the first sieving stage. Other fibers were classified as "residue fibers." The finest and finer fibers (desired fibers) that were recovered from the sieving process can be utilized for 3D printing purposes, whereas the residue fibers can be repurposed for other applications or can be reground for further use.

The 1st sieving process required up to 12 hours to produce 801.8g of the finest fibers, without any of the finer fibers being collected. The second sieving process took 7.5 hours and resulted in the collection of 301.9g of the finest fibers and 102.8g of the finer fibers. An additional 5.5 hours were required for the third sieving process, which yielded 82.4g of the finest fibers and 17.9g of the finer fibers. The remaining materials, totalling 1164.4g, were classified as residue fibers.

Three indicators were used to evaluate the effectiveness of sieving, i.e., percentage of different types of fibers in each sieving stage (%), recovery rate (%) and recovery speed (g/h). The percentage of desired fibers dropped significantly with each stage of sieving and during the fiber recovery process (Figure 5). This impact can be seen in the percentage of residue (fibers that were not recovered): For instance, after the 1st sieving, the percentage of residue was 66.2%. However, after the 3rd sieving, this percentage increased to 91.4%. The percentage of the finest fibers in each sieve displays a noticeable reduction, and the rate of this reduction becomes more pronounced.
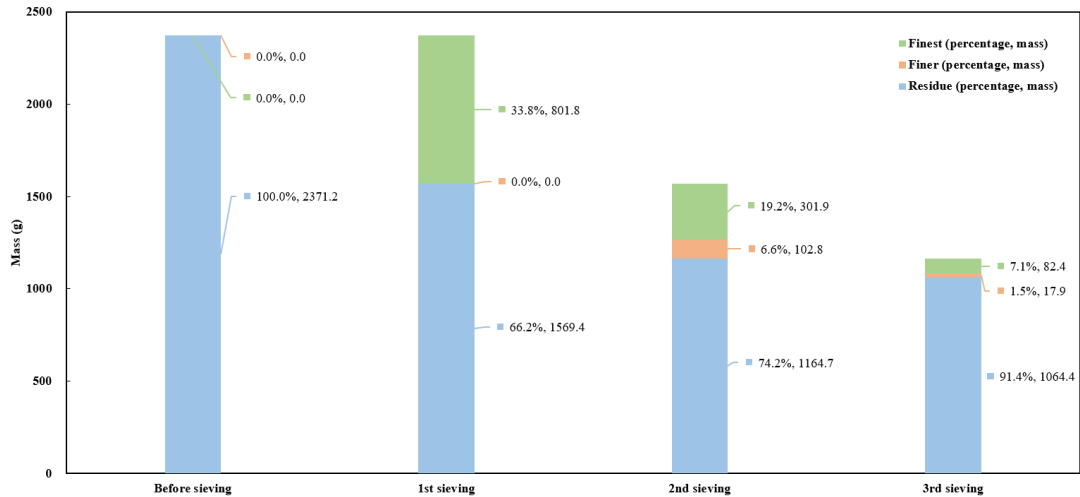
Figure 5: Distribution of different types of fibers after each sieving stage.

From the ground material, roughly 50% of the finest fibers and 5% of the finer fibers were recovered, resulting in an overall recovery rate of 55% (Figure 6). Interestingly, the third sieving stage had the lowest contribution to the overall recovery, with only 3.5% for the finest fibers and 0.5% for the finer fibers. Considering these findings, it was concluded that removing the third sieving stage could enhance the sieving efficiency.

As the sieving process progressed, the recovery rates of the finest and finer fibers showed a steady decline (Figure 7). However, the cumulative sieving time did not decrease uniformly, due to the diminishing number of fibers that could be collected with each successive sieving. This led to a non-linear reduction in the cumulative sieving time.
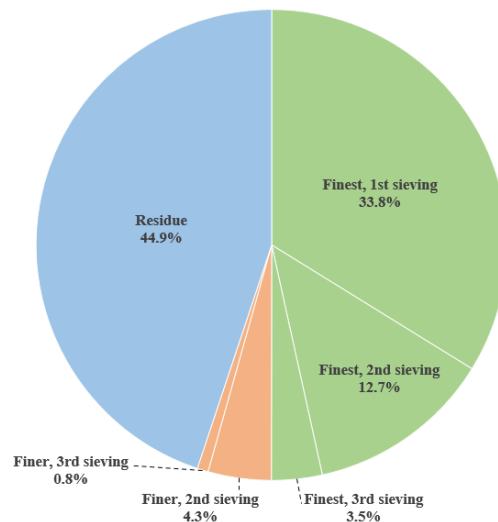
Figure 6: Ratios of different types of fibers after sieving.

It should be noted that the sieving process can be optimized by controlling the material fill level in the screen, preventing the formation of dense layers of short fibers, which hinder the recovery of fibers in the upper layer. That being said, it is important to avoid fully filling the screen with the material during the first sieving process, since the unsieved material contains fibers of varying lengths. As the

second or third sieving is performed, some short fibers have been removed, and more long fibers remain in the screen, leaving larger gaps between them. This allows the short fibers to pass through these gaps. As a result, approximately 70%, 80%, and 90% of the maximum screen content of fibers were added in the first, second, and third sieving, respectively. The average sieving speed is approximately steady at 200g/h.
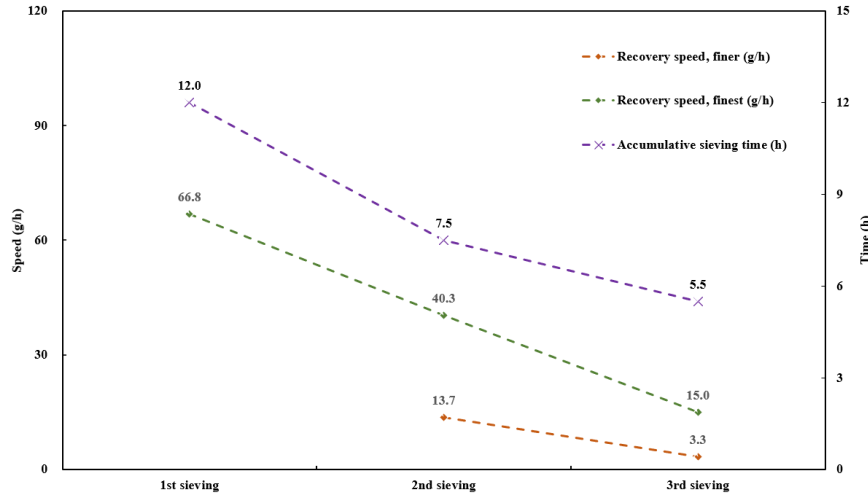

Figure 7: Recovery speed and accumulative sieving time of each sieving stage.

Several key findings emerged from the sieving work conducted as part of the study. The optimal sieving time was determined to be 30 minutes based on the observed fiber recovery rates and sieving efficiency. In total, 55% of the original fiber mass was effectively recovered for use in 3D printing through the grinding and sieving process. While the secondary sieving processes were found to be necessary, the cost of additional sieving (such as a third round) was not justified. Additionally, the speed of effective fiber recovery decreased notably as the number of sieving processes increased. Finally, optimizing the sieving process can be achieved by regulating the material fill level in the screen.

2.2 Filament extrusion

After the initial grinding process, a mixture of fibers from turbine blade waste and PLA pellets (Ingeo 4043D, Natureworks LLC, Blair, Nebraska) underwent a dehydrating process for four hours at 60°C to bring the moisture content of the pellets below 250 ppm. The dehydrated mixture was then fed into a twin-screw extruder (Leistritz ZSE18HP-40D, Nuremberg, Germany) with 8 subzones and a pelletizer, resulting in glass fiber-reinforced pellets. The produced pellets were dried again and fed into a single screw extruder (FilaFab, D3D Innovations Limited, Bristol, UK) to manufacture glass fiber-reinforced filaments with a diameter of 1.75±0.05 mm. The diameter of the filaments was constantly monitored by a laser micrometer with an accuracy of ±2 μm during extrusion. The specifications of the twin-screw and single extruders are presented in Table 1.

Specimens of glass fiber-reinforced material were printed using a 3D printer Prusa i3 Mk2S with a total thickness of 3.36 mm and a $[0]_{24}$ stacking sequence after the filaments were produced. Specific manufacturing and design parameters for the printing of the specimens are listed in Table 2.

	Screw speed (rpm)	90
	Subzone 1-2 (Temp., °C)	190
	Subzone 3(Temp., °C)	185
Twin screw pelletizer	Subzone 4 (Temp., °C)	180
	Subzone 5 (Temp., °C)	175
	Subzone 6-8 (Temp., °C)	170
	Screw speed (rpm)	25
Single screw filament maker	Die temperature (Temp., °C)	210
	Winder speed (rpm)	1

Table 1: The parameters of twin-screw and single extruders.

Manufacturing parameter	Value	Manufacturing parameter	Value
Print direction	XYZ	Nozzle diameter (mm)	0.4
Raster angle (°)	0	Nozzle temperature (°C)	215
Layer height (mm)	0.14	Cooling	N.A.
Bed temperature (°C)	60	Infill (%)	100
Print speed (mm/min)	2400	Filament diameter (mm)	1.75

Table 2: Manufacturing and design parameters for specimen 3D printing.

3 MICROMECHANICAL FE ANALYSIS

3.1 Generation of RVEs

Three fundamental concepts are necessary to predict the elastic properties of recycled 3D printed parts for FE analysis. Firstly, it is important to create distinct hierarchical orders that accurately represent the macrostructure of the 3D-printed parts. Secondly, the elastic properties of randomly distributed fibers within a cubic RVE can be evaluated using the homogenization method. Finally, the structural stiffness and Poisson's ratios of 3D printed parts can be assessed by formulating the homogenization problem on the 3D printing building block. These concepts are crucial to accurately predict the elastic properties of recycled 3D printed parts and are therefore essential to the FE analysis.

3.1.1. Generation of RVE cuboid

The size of the RVE cubic volume is determined based on sensitivity analysis and comparison with experimental data, as well as previous studies that suggest a minimum RVE length of twice the average fiber length for satisfactory results [20]. It should be noted that this conclusion was made under the assumption that all fiber lengths are identical, which is not the case in the current recycling method. Therefore, the length of fibers, as well as their distribution, is important for accurate results.

3.1.2. Generation of fibers

To model the fibers in the FE analysis, they are assumed to be straight cylinders with circular cross-sections and a constant radius. This assumption is based on the small aspect ratios, low volume fraction [20], and negligible impact of a non-constant radius on the elastic properties [21]. The radius of the cylinders is set as the mean value of the actual fiber radius obtained from experimental measurements. The range of fiber lengths is determined based on the classification operation illustrated in Figure 8.
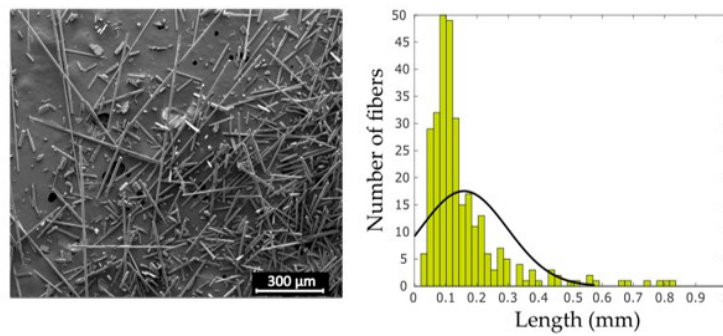
Figure 8: SEM image of fibers and fiber length distribution [11, 22].

Several variables are necessary to describe the state of fibers in the RVE cuboid, such as the fibers' position determined by a random function, the length chosen from the length range of recycled fibers, the radius, and two orientation angles. The fiber orientations are classified into two groups based on their predominance in a single direction (UD group) or random directions (RD group) as observed in experiments (Figure 9). Moreover, the RVE frame must not contain any fiber intersection as it is physically unacceptable. To ensure the geometry's periodicity, the fiber parts that penetrate the RVE frame's exterior surface are translated to the opposite side (face) inside the RVE frame.
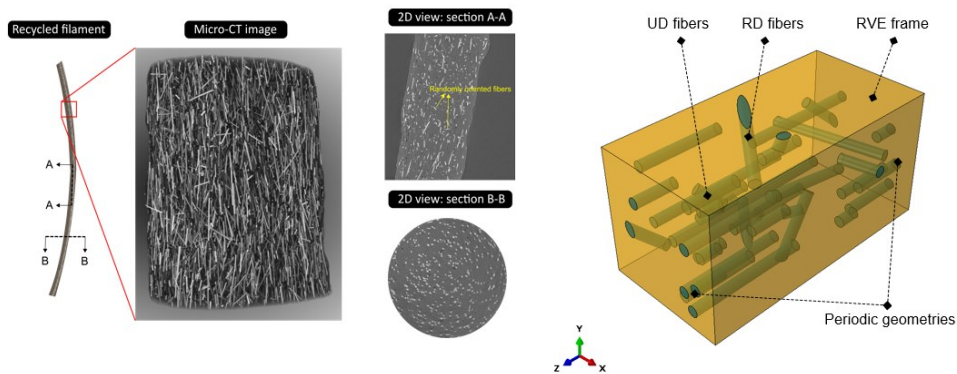

Figure 9: The micro-computed tomography (CT) scan of recycled fabricated filament and corresponding RVE.

The modified random sequential adsorption (MRSA) algorithm, which is used to generate the fibers, is implemented using ABAQUS CAE and PYTHON scripts. This algorithm is an improvement over classic RSA algorithms as it eliminates redundant calculations required to check for fiber intersections. In the classic RSA algorithm, each newly generated fiber needs to be tested against all previously accepted fibers, leading to a time-consuming process. In contrast, the MRSA algorithm only requires one bulk calculation, as shown in Figure 10. Furthermore, the MRSA algorithm overcomes the limitation of generating fibers for arbitrary geometries and has fewer misjudgements in cases where one fiber end is almost in contact with another fiber.
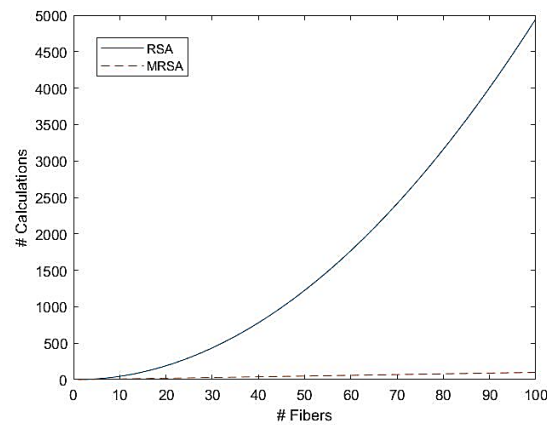
Figure 10: Number of calculations required for RSA and MRSA to check fiber intersections.

3.2 Homogenization

Once the MRSA algorithm has completed the generation of fibers, it will continue until the RVE with the desired entities is achieved (Figure 11). The data of the reinforcement states are then exported to reconstruct, mesh, and analyze the 3D problem of randomly distributed recycled fiber composites. The composites are modelled using 10-node quadratic tetrahedron elements (C3D10). To ensure periodic boundary conditions (PBC) with non-periodic meshes, an interpolation technique is used, which is implemented into the EasyPBC plugin tool [23].
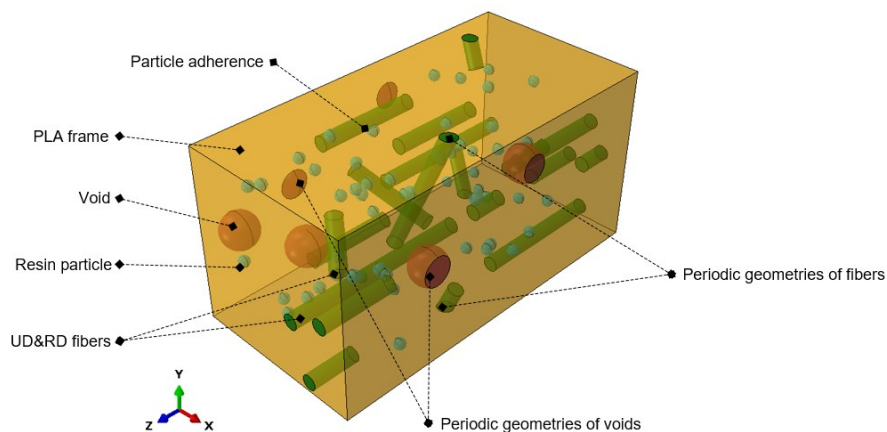

Figure 11: RVE hierarchical structure of recycled glass fiber reinforced specimen.

4   RESULTS AND DISCUSSION

In this study, the procedures were employed to perform FE analysis of 3D-printed recycled composite components, made from PLA and recycled glass fibers. To obtain the properties of the fibers, a single fiber tensile test was conducted on fibers that were extracted from the ground using wind turbine blades [12]. The assigned Young's modulus and Poisson's ratio for the matrix and fibers were $E_m = 3.6$ GPa, $v_m = 0.33$; $E_f = 75$ GPa, $v_f = 0.22$, respectively. The mechanical properties of the components were predicted using FE and mechanical theories of short fiber composites, based on the actual fiber content of the filaments that were determined via Thermogravimetric Analysis (TGA).

The mechanical behaviour of a composite material is greatly influenced by the proportion of its

constituents, with the fibers having the most significant impact on the overall performance compared to other inclusions such as resin particles and voids. In this study, the mechanical properties of 3D printed specimens were evaluated by varying the fiber content in three different proportions: 0%, 5%, and 10% by weight. The obtained numerical results and experimental data are depicted in Figure 12.

The stiffness in the direction of the leading fiber distribution (referred to as the 3-direction) is an important design parameter for composite materials. The stiffness values in the 3-direction obtained through finite element (FE) and micromechanical models were found to be in good quantitative agreement with the experimental measurements. Compared to analytical models like Mori-Tanaka and Halpin-Tsai, the use of realistic model details in the Representative Volume Element (RVE) model effectively reduced errors with the experimental results. However, the FE results still showed an overestimation in all fiber content scenarios, indicating the need for proper minimization of intrinsic and extrinsic defects and voids, which are the leading causes of property degradation in short fiber samples.
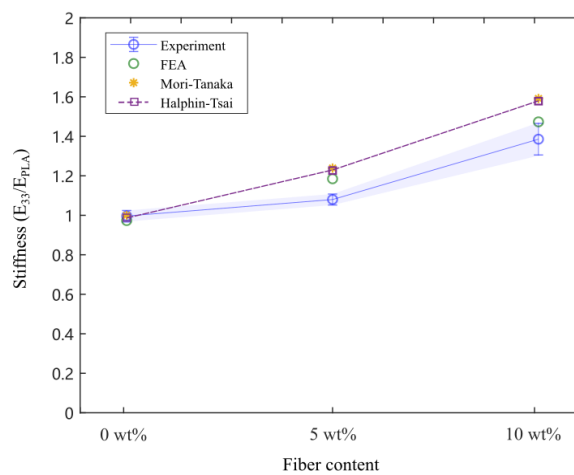

Figure 12: Normalized stiffness of 3D printed specimens from FE, analytical, and experiments.

5   CONCLUSIONS

This study presents a promising recycling method for wind turbine waste using mechanical grinding and fused filament fabrication. The sieving process of the recycled glass fibers was studied, and potential optimizations were explored.

Key findings from the sieving indicate:

(1) A 30-minute sieving time provides a balance between fiber recovery rate and sieving efficiency.

(2) The recovery rate of fibers suitable for 3D printing with a nozzle diameter of 0.4 mm is 55%.

(3) The double sieving process is an effective method for extracting more desired fibers, while a third sieving process is found to have a low necessity.

Furthermore, an RVE model using an MRSA algorithm was applied to simulate the mechanical behaviour of 3D-printed recycled parts. The MRSA algorithm has facilitated the generation of RVEs with hybrid arbitrary-geometry reinforcements, and FE analysis has validated the mechanical properties of 3D-printed specimens with recycled materials. The RVE model has the potential to optimize the design of 3D-printed specimens.

ACKNOWLEDGEMENTS

REFERENCES

[1]   J. Chen, J. Wang, and A. Ni, "Recycling and reuse of composite materials for wind turbine blades: An overview," *Journal of Reinforced Plastics and Composites,* vol. 38, no. 12, pp. 567-577, 2019.

[2]   D. S. Cousins, Y. Suzuki, R. E. Murray, J. R. Samaniuk, and A. P. Stebner, "Recycling glass fiber thermoplastic composites from wind turbine blades," *Journal of cleaner production,* vol. 209, pp. 1252-1263, 2019.

[3]   L. Mishnaevsky, K. Branner, H. N. Petersen, J. Beauson, M. McGugan, and B. F. Sorensen, "Materials for Wind Turbine Blades: An Overview," (in eng), *Materials (Basel),* vol. 10, no. 11, Nov 9 2017, doi: 10.3390/ma10111285.

[4]   H. Albers, S. Greiner, H. Seifert, and U. Kühne, "Recycling of wind turbine rotor blades. Fact or fiction?; Recycling von Rotorblaettern aus Windenergieanlagen. Fakt oder Fiktion?," *DEWI-Magazin,* 2009.

[5]   K. Larsen, "Recycling wind turbine blades," *Renewable energy focus,* vol. 9, no. 7, pp. 70-73, 2009.

[6]   S. A. Martin, "Comparison of hammermill and roller mill grinding and the effect of grain particle size on mixing and pelleting," 1985.

[7]   J. Palmer, O. R. Ghita, L. Savage, and K. E. Evans, "Successful closed-loop recycling of thermoset composites," *Composites Part A: Applied Science and Manufacturing,* vol. 40, no. 4, pp. 490-498, 2009.

[8]   G. Schinner, J. Brandt, and H. Richter, "Recycling carbon-fiber-reinforced thermoplastic composites," *Journal of Thermoplastic Composite Materials,* vol. 9, no. 3, pp. 239-245, 1996.

[9]   T. Inoh, T. Yokoi, K.-I. Sekiyama, N. Kawamura, and Y. Mishima, "SMC recycling technology," *Journal of Thermoplastic Composite Materials,* vol. 7, no. 1, pp. 42-55, 1994.

[10]   M. Roux, C. Dransfeld, N. Eguémann, and L. Giger, "Processing and recycling of a thermoplastic composite fibre/peek aerospace part," in *Proceedings of the 16th European conference on composite materials (ECCM 16)*, 2014, pp. 22-26.

[11]   A. Rahimizadeh, J. Kalman, K. Fayazbakhsh, and L. Lessard, "Recycling of fiberglass wind turbine blades into reinforced filaments for use in Additive Manufacturing," *Composites Part B,* vol. 175, 2019, doi: 10.1016/j.compositesb.2019.107101.

[12]   M. Tahir, A. Rahimizadeh, J. Kalman, K. Fayazbakhsh, and L. Lessard, "Experimental and analytical investigation of 3D printed specimens reinforced by different forms of recyclates from wind turbine waste," *Polymer Composites,* vol. 42, no. 9, pp. 4533-4548, 2021, doi: 10.1002/pc.26166.

[13]   S. Kari, H. Berger, and U. Gabbert, "Numerical evaluation of effective material properties of randomly distributed short cylindrical fibre composites," *Computational Materials Science,* vol. 39, no. 1, pp. 198-204, 2007, doi: 10.1016/j.commatsci.2006.02.024.

[14]   T. Mori and K. Tanaka, "Average stress in matrix and average elastic energy of materials with misfitting inclusions," *Acta metallurgica,* vol. 21, no. 5, pp. 571-574, 1973.

[15]   B. D. Agarwal, L. J. Broutman, and K. Chandrashekhara, *Analysis and performance of fiber composites*. John Wiley & Sons, 2006.

[16]   L. T. Harper, T. A. Turner, N. A. Warrior, and C. D. Rudd, "Characterisation of random carbon fibre composites from a directed fibre preforming process: The effect of fibre length," *Composites Part A: Applied Science and Manufacturing,* vol. 37, no. 11, pp. 1863-1878, 2006, doi: 10.1016/j.compositesa.2005.12.028.

[17] L. T. Harper, T. A. Turner, N. A. Warrior, and C. D. Rudd, "Characterisation of random carbon fibre composites from a directed fibre preforming process: The effect of tow filamentisation," *Composites Part A: Applied Science and Manufacturing,* vol. 38, no. 3, pp. 755-770, 2007, doi: 10.1016/j.compositesa.2006.09.008.

[18] S. Arabnejad and D. Pasini, "Mechanical properties of lattice materials via asymptotic homogenization and comparison with alternative homogenization methods," *International Journal of Mechanical Sciences,* vol. 77, pp. 249-262, 2013.

[19] R. Hill, "Elastic properties of reinforced solids: some theoretical principles," *Journal of the Mechanics and Physics of Solids,* vol. 11, no. 5, pp. 357-372, 1963.

[20] W. Tian, L. Qi, J. Zhou, J. Liang, and Y. Ma, "Representative volume element for composites reinforced by spatially randomly distributed discontinuous fibers and its applications," *Composite Structures,* vol. 131, pp. 366-373, 2015, doi: 10.1016/j.compstruct.2015.05.014.

[21] A. A. Gusev, P. J. Hine, and I. M. Ward, "Fiber packing and elastic properties of a transversely random unidirectional glass/epoxy composite," *Composites Science and Technology,* vol. 60, no. 4, pp. 535-541, 2000.

[22] A. Rahimizadeh, J. Kalman, R. Henri, K. Fayazbakhsh, and L. Lessard, "Recycled Glass Fiber Composites from Wind Turbine Waste for 3D Printing Feedstock: Effects of Fiber Content and Interface on Mechanical Performance," *Materials,* vol. 12, no. 23, p. 3929, 2019. [Online]. Available: https://www.mdpi.com/1996-1944/12/23/3929.